

# INTERFACE HEAT TRANSFER AND THERMAL ACCOMMODATION COEFFICIENTS: HEATED TUNGSTEN WIRE IN NITROGEN ENVIRONMENT

S. H. P. CHEN and S. C. SAXENA

Department of Energy Engineering, University of Illinois at Chicago, Chicago, Illinois 60680, U.S.A.

(Received 18 December 1972 and in revised form 2 July 1973)

**Abstract**—An experimental facility of the general hot-wire type is described for the study of interface heat transfer from heated metal surfaces to the surrounding gas environment with a view to probe into the different molecular mechanisms of energy transport which are established by the successive reduction of the test gas pressure. In particular, this initial effort reports the measured heat transfer rates from tungsten, heated up to a maximum temperature of 1450°K, in nitrogen at different pressure levels in the range 0.8 to about 30 cm of mercury. The heat transfer data taken in the temperature-jump region are interpreted in three alternative ways. The temperature-jump theory is successfully checked by computing and comparing the thermal conductivity values obtained as a function of temperature from data taken within as well as outside the temperature-jump region. The thermal accommodation coefficients are thus obtained for nitrogen on a tungsten surface with an adsorbed film of mostly nitrogen in the temperature range 450°–1450°K, and these exhibit a weak minimum or dip at about 850°K. These data will thus serve an important engineering design need because the experimental conditions correspond to the configuration most often encountered in practice.

## NOMENCLATURE

|             |   |             |   |
|-------------|---|-------------|---|
| $a$ ,       | radius of the tungsten wire [cm];   | $r$ ,       | radial coordinate [cm];   |
| $a_p$ ,     | constant in equation (8) [mW/m deg K];  | $R$ ,       | gas constant [erg/g mole deg K];  |
| $A$ ,       | constant in equation (1) [(deg C) <sup>-1</sup> ];  | $R_0$ ,     | resistance per unit length of the wire at the ice temperature [ohm/cm]; |
| $b$ ,       | inner radius of the column glass wall [cm];   | $R_p$ ,     | resistance per unit length of the wire at a temperature $t$ [ohm/cm];   |
| $b_p$ ,     | constant in equation (8) [mW/m (deg K) <sup>2</sup> ];  | $t$ ,       | temperature [deg C];  |
| $B$ ,       | constant in equation (1) [(deg C) <sup>-2</sup> ];  | $T$ ,       | temperature [deg K];  |
| $C_v$ ,     | specific heat at constant volume [erg/g mol deg K];   | $\bar{T}$ , | mean temperature of the gas [deg K];                                    |
| $g$ ,       | temperature jump distance [cm];   | $T_e$ ,     | linearly extrapolated gas temperature on the wire surface [deg K];      |
| $k$ ,       | thermal conductivity of gas [mW/m deg K];   | $T_H$ ,     | wire temperature [deg K];   |
| $\bar{k}$ , | thermal conductivity of gas at its average temperature [mW/m deg K];                                    | $T_{L_1}$ , | gas temperature at $L_1$ [deg K];                                       |
| $2L$ ,      | length of the tungsten wire [cm];   | $T_{L_n}$ , | gas temperature at $L_n$ [deg K];                                       |
| $L_{1p}$ ,  | a distance of one mean-free-path away from the tungsten wire [cm];                                      | $T_w$ ,     | column glass wall temperature [deg K];                                  |
| $L_{1p}$ ,  | a distance of one mean-free-path away from the glass wall [cm];   | $w$ ,       | thickness of the column glass wall [cm];                                |
| $M$ ,       | molecular weight of the gas [g/mole];   | $\alpha$ ,  | accommodation coefficient of the gas and the solid surface.             |
| $P$ ,       | gas pressure [cm Hg];   |             |   |
| $Q_H$ ,     | thermal power propagated through the gas in the presence of jump-effect [W];                            |             |   |
| $Q_T$ ,     | thermal power fed to the wire in the presence of gas [W];   |             |   |
| $Q_v$ ,     | thermal power fed to the wire in vacuum [W];  |             |   |
| $Q_{HKT}$ , | thermal power propagated through the gas which is in thermal equilibrium with the hot-wire surface [W]. |             |   |

## INTRODUCTION

THE KNOWLEDGE of thermal accommodation coefficients (hereafter abbreviated as A.C.'s) of gases at metal surfaces is basic to the understanding of a wide variety of such phenomena as adsorption, catalysis, energy transfer at an interface, thermal energy relaxation, gas-surface interaction potentials, etc. The available information on A.C.'s is quite limited as evident from the critical reviews of Vines [1], Hart-

nett [2], and Wachman [3]. There are practically no measurements above 500°K, and in spite of several efforts [4–11] following the pioneer work of Devonshire [12], our theoretical capability has not yet reached a state where reliable *ab initio* calculations may be possible even for noble gases on well-defined metal surfaces. Consequently, direct reliable measurements of A.C.'s over an extended temperature range will be very useful for practical engineering needs and these will also help in an important way in the development of a theory which may enable calculations of A.C.'s from first principles.

Here, we describe a general hot-wire type facility appropriate for the measurement of heat transfer rates from the metal surfaces as a function of its temperature into gases at various pressures. In particular, we report results for tungsten wires with an adsorbed gas film, which is heated in steps from 450° to 1450°K in 99.9995 per cent pure nitrogen environment in three different heat transfer hot-wire columns. The nitrogen gas is stated to have trace impurities of O<sub>2</sub>, H<sub>2</sub>, Ar, He and Ne which are less than 1 part per million and of CO<sub>2</sub> and CH<sub>4</sub> which are less than 0.5 part per million. The sample is quoted to have no CO. The nitrogen pressure in each case and at each temperature is varied in the range 0.8 to about 30 cm of mercury. These steady state experimental data are pooled together in conjunction with the theory of heat transfer rate from a heated wire in a gas in the temperature-jump region, and the A.C.'s are computed as a function of temperature.

The kinetic theory interpretation of the temperature-jump phenomenon as given in recent years [13, 14] enables the calculation of A.C.'s from the experimental data under well-defined approximations. We discuss three different procedures of treating the data and point out their relative usefulness. The heat transfer data obtained in the low pressure region is particularly not appropriate at high temperatures because of the increasing outgassing [15] and radiation [2]. From a practical standpoint, after the test metal surface is prepared as desired, the chances of altering any adsorbed film on the wire are much larger in the low pressure method than in the temperature-jump regime. In the latter case the metal surface will invariably be saturated with the gas and just from the engineering point of view this configuration where the metal surface is always covered with the test gas film will more appropriately accord to the conditions encountered in many real situations. However, the heat transfer rates measured in the low-pressure range can with suitable precautions be approximated quite

closely to a pure metal surface and test gas interface, a configuration which is more interesting from the theoretical point of view. These are only qualitative guides and each practical situation will need a careful detailed individual examination. However, the existing limited experimental data do indicate that the results of A.C.'s as obtained from the slip-flow condition in the temperature-jump region and the free-molecule flow in the low pressure region are in good agreement with each other, Thomas and Golike [16], Wachman [3]. We hope to shed further light on this important point in the future as our measurements are completed over a still extended temperature range and to include other gases.

## EXPERIMENTATION

The principal component of the experimental arrangement is the heat transfer column shown in Fig. 1. Three such columns of dimensions given in

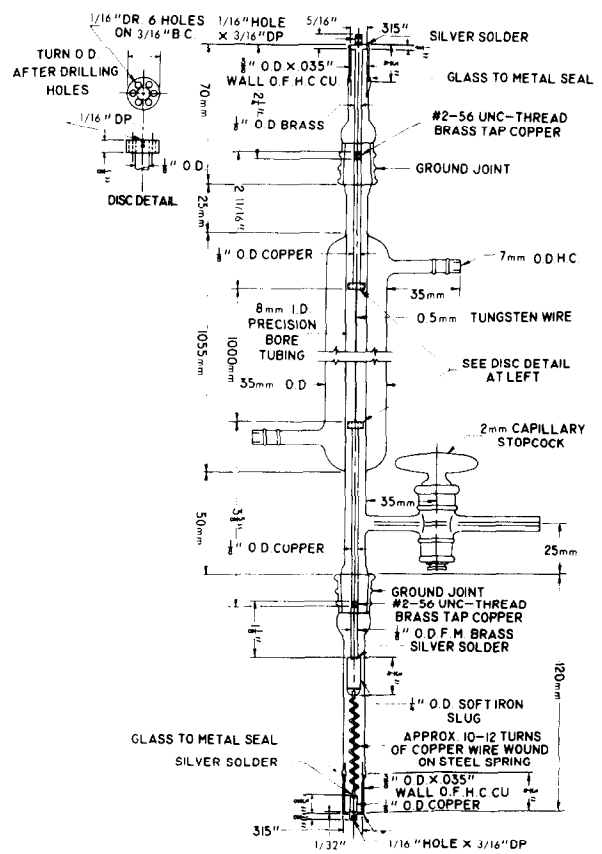


FIG. 1. A typical schematic of the heat transfer column, not to the scale.

Table 1. Dimensions (cm) of the heat transfer columns and the range of test gas pressures (cm of mercury)

| Column and data set number |                                   |   |   |
|----------------------------|-----------------------------------|---|---|
| 2L                         | 92.13                             | 92.80   | 53.93                                   |
| 2b                         | 0.800                             | 0.800   | 0.800                                   |
| 2a                         | 0.03048                           | 0.05080   | 0.05080                                 |
| W                          | 0.208                             | 0.208   | 0.208                                   |
| P                          | 2.0, 5.0, 11.0,<br>20.2, and 30.2 | 0.8, 1.1, 1.2,<br>1.4, 1.6, 3.1,<br>10.1 and 21.1 | 0.8, 1.0, 1.6,<br>3.3, 10.2 and<br>20.0 |

Table 1 are used in the present series of measurements. The glass column wall is maintained at a constant temperature by circulating water through the jacket at  $30.0 \pm 0.02^\circ\text{C}$  from a Haake model FS constant temperature circulator. The tungsten wire is mounted axially in the column with a high degree of precision and is kept taut over the entire temperature range by providing adequate pull through a steel spring and a soft iron weight. The column is evacuated to a lowest pressure of  $2 \times 10^{-7}$  torr with a high vacuum system supplied by Heracus-Engelhard Vacuum, Inc. The column is charged with the test gas from a connected, properly designed, glass gas handling manifold and its pressure is measured on a mercury manometer and cathetometer arrangement to an accuracy of  $\pm 0.001$  cm. The tungsten wire is heated to different temperatures by passing current from three Hewlett-Packard 6274A D.C. power supplies. The steady electric potentials are monitored on a Hewlett-Packard model 3450A multi-function meter and are finally measured on a Leeds and Northrup 7556 six-dial guarded precision potentiometer and related accessories.

The tungsten wire is also used as its own thermometer. The electrical resistance of a given sample of wire is measured at the ice point, and at the melting points of zinc ( $419.51^\circ\text{C}$ ) and aluminum ( $660.37^\circ\text{C}$ ) in a Leeds and Northrup 8411 fixed-temperature facility. In this temperature range, the resistance of the tungsten wire,  $R_t$ , at a temperature of  $t^\circ\text{C}$  is related to its resistance at  $0^\circ\text{C}$ ,  $R_0$ , by the following quadratic relation, Davis [17],

$$R_t = R_0(1 + At + Bt^2). \quad (1)$$

The wire temperature is also measured with a pyro micro-optical pyrometer, Model M-6018, supplied by the Pyrometer Instrument Co. of New Jersey. The stated maximum uncertainties are within  $\pm 4^\circ$  in the range 1100–1600°K. The temperatures extrapolated on the basis of equation (1) and those determined with the pyrometer agree with each other within

about one per cent up to about  $1600^\circ\text{C}$ . We have preferred to determine temperatures over the whole range on the basis of equation (1). Chemically cleaned and straightened tungsten wires, supplied by General Electric, are used. The wires are carefully annealed in vacuum and it is found that such a wire has a reproducible resistance versus temperature characteristic. This check is repeatedly made when different series of measurements are taken over the same specimen of wire ranging over several months. The constants of equation (1) for an annealed wire as determined from fixed temperature resistance measurements are reported in Table 2.

Table 2. Constant  $R_0$ ,  $A$  and  $B$  of equation (1) for tungsten wires

| Wire diameter<br>(mm) | $R_0$<br>(m ohm $\text{cm}^{-1}$ ) | $A \times 10^3$<br>(deg $\text{C}^{-1}$ ) | $B \times 10^6$<br>(deg $\text{C}^{-2}$ ) |
|-----------------------|------------------------------------|---|---|
| 0.3048                | 7.903                              | 4.265                                     | 0.7651                                    |
| 0.5080                | 2.901                              | 3.913                                     | 0.8260                                    |

A typical run consists in evacuating the heat transfer column and then in determining the power  $Q_v$ , required to heat the wire of a known length to different temperatures,  $T_H$ . Next, the test gas is transferred at the desired pressure and the electrical measurements are repeated to determine the power  $Q_T$  necessary to heat the same wire to different temperatures in the same range. The length of the wire is monitored on a cathetometer within  $\pm 0.001$  cm. The increase of gas pressure during a run is noted on a mercury manometer, but its variation due to changes in the wire temperature is ignored in calculations. The maximum relative change in pressure is about 1.2 per cent at the highest temperature (about  $1000^\circ\text{C}$ ) and at the lowest gas pressure (about 8 mm of mercury). Various sets of  $Q_v$  and  $Q_T$  measurements are taken with wires of different lengths and diameters and in each case at a series of gas pressures, the specific values are listed in Table 1. Let us represent the thermal power propagated through the gas by

$$Q_T - Q_v = Q_H. \quad (2)$$

It may be pointed out that before starting a series of measurements the heat transfer column is evacuated and the wire is heated in steps up to the highest temperature of  $2500^\circ\text{K}$  and maintained at this temperature for several hours while the column is still connected to the high vacuum pumping system. The wire is then cooled slowly to the room tempera-

ture in vacuum and the measurements of  $Q_v$  and  $Q_T$  at a fixed test gas pressure are resumed. We [18, 19] have already shown by experimental and analytical investigations that under such conditions the thermal energy transport by convection and end effects is negligibly small compared to  $Q_T$ , and the latter are confined over a small end region of the column. Further, that  $Q_H$ , determined by the difference of  $Q_T$  and  $Q_v$ , will appropriately represent the net energy transport by the test gas molecules is also substantiated by the work of Saxena and Davis [20].

If the gas pressure in the column is such that the mean-free-path is of the order of the wire diameter, the impinging molecules on the wire surface under this condition will not acquire or accommodate to its temperature, and an appreciable temperature discontinuity at the interface is created [21, 22]. The effect of a similar discontinuity at the gas-glass (cold wall) interface is relatively small on the thermal energy transport for the geometrical configuration under discussion and will be consistently neglected in this work. If the extrapolated gas temperature at the hot-wire surface at  $T_H$  is  $T_e$ , then:

$$T_H - T_e = -g(\partial T/\partial r)_{r=a} \quad (3)$$

Here  $g$  is referred to as the temperature-jump distance;  $r$ , the radial coordinate;  $a$ , the radius of the tungsten wire; and,  $T$ , the temperature. Harris [14] developed a mean-free-path kinetic theory for the temperature distribution in a monatomic gas close to the hot-wire surface and derived an explicit relation between  $T_e$  and  $T_H$  under well-defined approximations. His final expression, further simplified for application to our experimental arrangement, is:

$$T_H - T_e = (Q_H/4\pi aLP)(\pi MT_e/2R)^{\frac{1}{2}} [(2 - \alpha)/2\alpha]. \quad (4)$$

Here,  $2L$  is the length of the tungsten wire;  $P$ , the test gas pressure;  $R$ , the gas constant;  $M$ , the molecular weight; and,  $\alpha$ , the A.C., is defined as the ratio of the actual rate of heat transfer from the wire surface to the gas to that which would exist if gas molecules striking the surface were re-emitted as if from a gas in equilibrium at the surface temperature. The relation of equation (4) is actually a polynomial in  $(1/P)$  but the next higher term is less than 1.5 per cent of the leading first term so that discussion of the results on the basis of this equation may be regarded as completely satisfactory. If  $Q_H$  is held constant for a given wire, the temperature distribution in the bulk of the gas, and hence  $T_e$ , will be independent of gas pressure. More explicitly, the reason for this lies in the fact that under these conditions the heat transfer from the wire is such that a

pressure dependent jump-effect is observed, while in the rest of the annulus the continuum heat flow condition exists. As the Fourier gas conductivity in this pressure range is independent of its pressure the temperature distribution in the bulk of the gas will also remain uninfluenced. Consequently, for this wire, a plot of  $T_H$  vs  $1/P$  for a constant value of  $Q_H$  will be linear with  $T_e$  as the intercept and will have a slope equal to  $(\pi MT_e/2R)^{\frac{1}{2}} [(2 - \alpha)/2\alpha] (Q_H/4\pi aL)$ . Hence, a combined knowledge of the intercept and slope will enable the determination of  $\alpha$  as a function of  $T_e$ . We have utilized this procedure which is referred to as the constant-power method.

If the Fourier relation is integrated under the assumption that the gas temperature at the filament  $T_e$  is given by equation (4), we get:

$$\frac{4\pi aL}{Q_H} = \frac{a \ln(b/a)}{\bar{k}(T_H - T_w)} + \frac{2 - \alpha}{2\alpha P} \left( \frac{\pi MT_e}{2R} \right)^{\frac{1}{2}} \frac{1}{(T_H - T_w)}. \quad (5)$$

Here,  $b$  is the inner radius of the glass column;  $\bar{k}$ , the thermal conductivity of the gas at its average temperature,  $T$ . The practical use of this equation presents additional difficulties and ambiguities. Specifically,  $T_e$  is often placed by  $T_H$ , and the identification of  $\bar{k}$  requires the knowledge of the temperature dependence of  $k$ . Thus, if  $k$  is assumed to vary linearly with temperature, equation (5) transforms to:

$$\frac{4\pi aL}{Q_H} = \frac{a \ln(b/a)}{k(\bar{T})(T_H - T_w)} + \frac{(2 - \alpha)}{2\alpha P} \left( \frac{\pi MT_e}{2R} \right)^{\frac{1}{2}} \frac{k(T_H)}{k(\bar{T})(T_H - T_w)}. \quad (6)$$

where  $\bar{T}$  is the arithmetic mean of  $T_H$  and  $T_w$ . Thomas and Golike [16] have given similar expressions for the two cases when  $k$  is proportional to  $T^{\frac{1}{2}}$  and  $T^{\frac{3}{2}}$ . According to equation (6), a plot of  $Q_H^{-1}$  vs  $P^{-1}$  for a constant value of  $T_H - T_w$  will be a straight line whose intercept will give  $k(\bar{T})$ , and the slope may be analyzed in terms of  $\alpha$  if adequate estimates of  $T_e$  and  $k(T_H)$  are made. This procedure of obtaining  $\alpha$  as a function of  $T_H$  is referred to as the constant temperature difference method. Further, the replacement of  $T_e$  by  $T_H$  in equation (6) is consistent with the use of equation (4) as long as terms containing higher powers of  $(1/P)$  than one are neglected. The latter assumption draws support from the experiments to be described in the next section.

Wachman [13] extended the scope of the mean-free-path theory, earlier employed in the low pressure region, in the temperature-jump region. He assumed that the gas molecules incident on the hot-wire surface are at a temperature  $T_{Lu}$  of the gas layer at a distance of one mean-free-path away from the wire

surface,  $L_1$ . Starting then from the relation for the A.C. similar to that which is used for the free molecular flow regime, viz.  $\alpha = Q_H/Q_{HKT}$ , he showed that for a monatomic gas:

$$\alpha = \left(\frac{\pi M}{2R}\right)^{\frac{1}{2}} \frac{Q_H T_{L_1}^{\frac{1}{2}}}{4\pi a L P (T_H - T_{L_1})} \quad (7)$$

$Q_{HKT}$  is the thermal power propagated through the gas when there is no temperature-jump at the hot-wire. It is consequently obtained by calculations based on equations derived from the kinetic theory.

Representing the temperature dependence of  $k$  by [23]

$$k(T) = a_1 + b_1 T \quad (8)$$

and disregarding the small thermal accommodation effect at the cold glass wall,  $T_{L_1}$  is obtained from the solution of the following relation:

$$T_{L_1} = \frac{a_1}{b_1} \left\{ \left[ 1 + \frac{2b_1}{a_1^2} \left( a_1 T_{L_1} + \frac{b_1}{2} T_{L_1}^2 + \frac{Q_H}{4\pi L} \ln \frac{b - L_{II}}{a + L_1} \right) \right]^{\frac{1}{2}} - 1 \right\} \quad (9)$$

where

$$T_{L_1}^{\frac{1}{2}} = \left(\frac{M}{128\pi R}\right)^{\frac{1}{2}} \frac{Q_H}{bLP} + \frac{1}{2} \left[ 4T_w + \frac{MQ_H^2}{32\pi RL^2 b^2 P^2} \right]^{\frac{1}{2}} \quad (10)$$

and  $L_{II}$  is a distance of one mean-free-path away from the cold glass wall.  $L_1$  and  $L_{II}$  are obtained on the basis of the simple kinetic theory expressions [21] and in conjunction with the literature data on density and viscosity of nitrogen. We have employed this mean-free-path method to determine  $\alpha$  as a function of  $T_{L_1}$ .

## RESULTS

Now we present an analysis of the three sets of data (Table 1) taken in the temperature-jump region and the values of  $\alpha$  so determined as a function of temperature according to the three procedures outlined in the previous section. In Fig. 2, the experimental data of sets I, II and III are plotted in accordance with equation (4). In each case  $T_H$  is seen to be linearly dependent on  $1/P$  for constant values of  $Q_H/4\pi aL$ , confirming thereby at least qualitatively the theory due to Harris [14].  $T_e$  and  $\alpha$  computed from the intercepts and slopes of these linear plots are given, respectively, in Table 3A and graphically displayed in Fig. 4A. In Fig. 3, these three sets of data are examined on the basis of equation (6) for the purpose of evaluating the constant temperature

difference method. These plots confirm the validity of the theory and indicate that for nitrogen, at least in the gas pressure range of 0.8–10 cm of mercury, the temperature-jump conditions exist. The corresponding range for the ratio of the tungsten wire diameter to the mean-free-path is 25–1000. The intercepts of these linear plots corresponding to  $1/P = 0$  may be utilized to determine  $k$  as a function of  $\bar{T}$ , and the values so obtained are reported in Table 4. The three sets of values are in fair agreement with each other, as well as with the values obtained from data taken

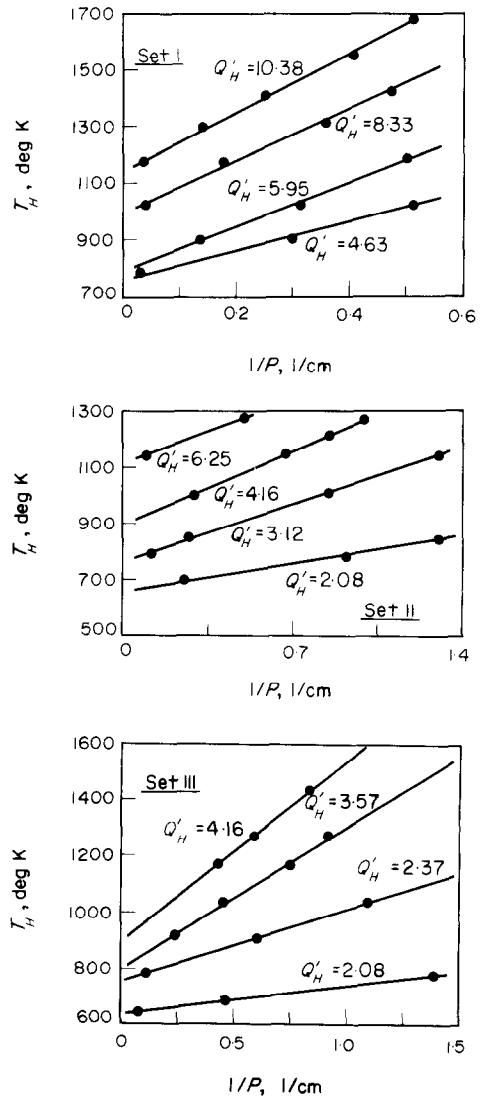


FIG. 2. Plots of  $T_H$  vs  $1/P$  for fixed values of  $(Q_H/4\pi aL) = Q'_H$  and for all the three sets of data. Constant power method, equation (4).

Table 3.  $\alpha$  for nitrogen on nitrogen-covered tungsten as a function of temperature ( $^{\circ}\text{K}$ )  
(A) Constant power method, equation (4)

| Set I |          | Set II |          | Set III |          |
|-------|----------|--------|----------|---------|----------|
| $T_e$ | $\alpha$ | $T_e$  | $\alpha$ | $T_e$   | $\alpha$ |
| 763   | 0.327    | 655    | 0.382    | 635     | 0.383    |
| 789   | 0.315    | 779    | 0.305    | 759     | 0.335    |
| 991   | 0.320    | 894    | 0.281    | 798     | 0.287    |
| 1144  | 0.337    | 1131   | 0.324    | 891     | 0.276    |

(B) Constant temperature difference method, equation (6)

| Set I |          | Set II |          | Set III |          |
|-------|----------|--------|----------|---------|----------|
| $T_H$ | $\alpha$ | $T_H$  | $\alpha$ | $T_H$   | $\alpha$ |
| 656   | 0.408    | 443    | 0.495    | 516     | 0.485    |
| 778   | 0.354    | 479    | 0.504    | 643     | 0.422    |
| 903   | 0.315    | 621    | 0.405    | 781     | 0.342    |
| 1020  | 0.347    | 693    | 0.387    | 915     | 0.319    |
| 1181  | 0.349    | 773    | 0.352    | 1042    | 0.365    |
| 1304  | 0.391    | 852    | 0.319    | 1161    | 0.367    |
| 1414  | 0.412    | 940    | 0.318    | 1278    | 0.395    |
|       |          | 1001   | 0.331    | 1445    | 0.406    |
|       |          | 1072   | 0.357    |         |          |
|       |          | 1142   | 0.364    |         |          |
|       |          | 1240   | 0.368    |         |          |
|       |          | 1276   | 0.377    |         |          |

(C) Mean-free-path method, equation (7)

| Set I<br>( $P = 2.0$ cm Hg) |           |          | Set II<br>( $P = 1.1$ cm Hg) |           |          | Set III<br>( $P = 1.6$ cm Hg) |           |          |
|-----------------------------|-----------|----------|------------------------------|-----------|----------|-------------------------------|-----------|----------|
| $T_H$                       | $T_{L_1}$ | $\alpha$ | $T_H$                        | $T_{L_1}$ | $\alpha$ | $T_H$                         | $T_{L_1}$ | $\alpha$ |
| 512                         | 497       | 0.454    | 653                          | 612       | 0.381    | 755                           | 714       | 0.326    |
| 1048                        | 956       | 0.310    | 850                          | 755       | 0.285    | 923                           | 808       | 0.281    |
| 1370                        | 1276      | 0.370    | 1270                         | 1115      | 0.350    | 1150                          | 1015      | 0.301    |

(D) Comparison of  $\alpha$  values obtained from different methods

| Temperature | Constant power method |          | Constant temperature difference method |          | Mean-free-path method |          |
|-------------|-----------------------|----------|--|----------|-----------------------|----------|
|             | eq. (4)               | eq. (4a) | eq. (6)                                | eq. (6a) | eq. (7)               | eq. (7a) |
| 450         | —                     | —        | 0.499                                  | 0.363    | —                     | —        |
| 550         | —                     | —        | 0.470                                  | 0.340    | 0.423                 | 0.282    |
| 650         | 0.380                 | 0.271    | 0.412                                  | 0.295    | 0.362                 | 0.241    |
| 750         | 0.329                 | 0.232    | 0.361                                  | 0.256    | 0.307                 | 0.205    |
| 850         | 0.290                 | 0.203    | 0.323                                  | 0.228    | 0.270                 | 0.180    |
| 950         | 0.298                 | 0.209    | 0.320                                  | 0.225    | 0.294                 | 0.196    |
| 1050        | 0.324                 | 0.228    | 0.345                                  | 0.244    | 0.321                 | 0.214    |
| 1150        | 0.348                 | 0.246    | 0.368                                  | 0.261    | 0.344                 | 0.229    |
| 1250        | —                     | —        | 0.381                                  | 0.271    | 0.368                 | 0.245    |
| 1350        | —                     | —        | 0.398                                  | 0.284    | 0.382                 | 0.255    |
| 1450        | —                     | —        | 0.417                                  | 0.299    | —                     | —        |

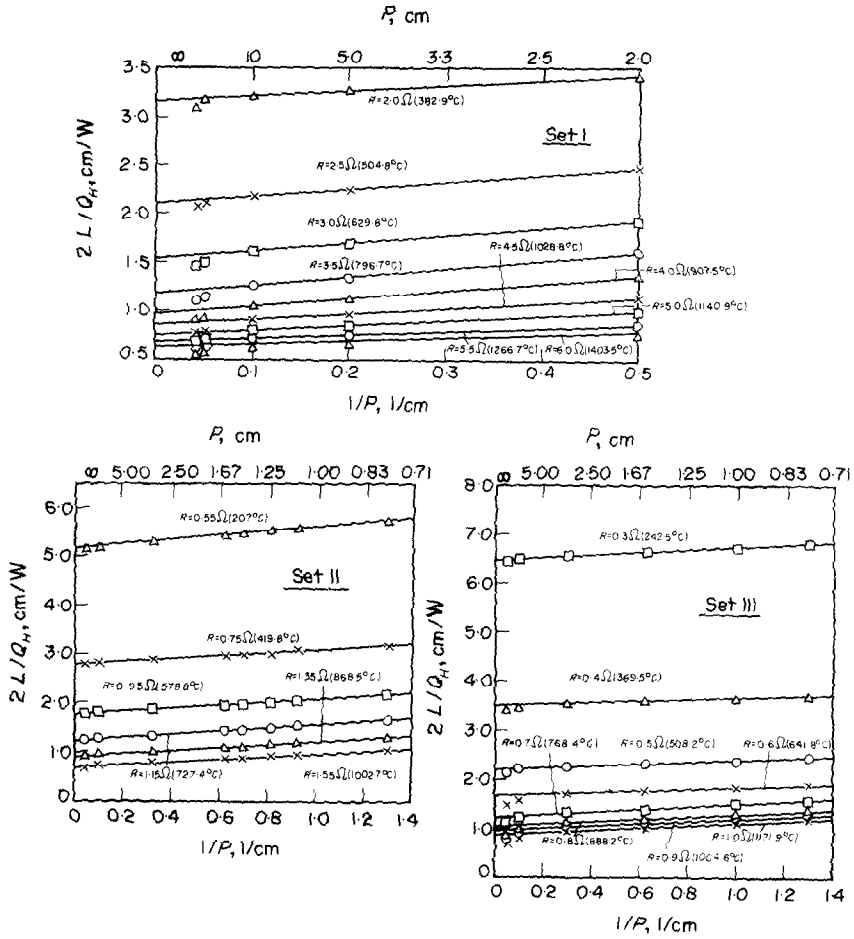


Fig. 3. Plots of  $2LQ_H^{-1}$  as a function of  $P^{-1}$  for the three sets of measurements. Constant temperature difference method, equation (6).

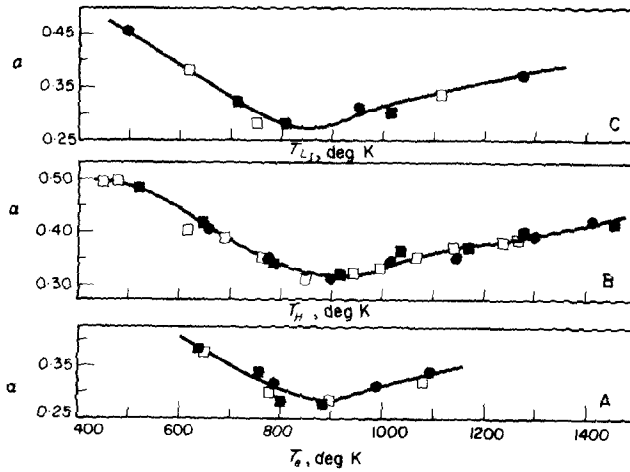


Fig. 4. Variation of  $\alpha$  with temperature: A, constant power method, B, constant temperature difference method, and C, mean-free-path method. ● Set I, □ Set II, and ■ Set III.

Table 4. Thermal conductivity values (mW/m deg K) of nitrogen determined from data taken in the temperature-jump region

| $t$<br>(°C) | Set I                                 | Set II | Set III | Mean high<br>pressure value<br>$P \approx 20$ cm Hg<br>and equation (11) | Set I                                  | Set II | Set III |
|-------------|---------------------------------------|--------|---------|--|--|--------|---------|
|             | Low pressure data and<br>equation (6) |        |         |  | Low pressure data and<br>equation (11) |        |         |
| 100         | 30.6                                  | 30.7   | 29.7    | 30.6   | 30.6                                   | 30.7   | 29.6    |
| 200         | 36.8                                  | 36.8   | 36.1    | 37.0   | 36.6                                   | 36.7   | 36.0    |
| 300         | 42.1                                  | 42.2   | 40.3    | 42.5   | 42.0                                   | 42.1   | 40.1    |
| 400         | 47.2                                  | 46.7   | 45.7    | 48.2   | 47.0                                   | 46.5   | 45.5    |
| 500         | 52.1                                  | 53.4   | 53.8    | 53.7   | 52.0                                   | 53.2   | 53.7    |
| 600         | 58.1                                  | 58.1   | 58.8    | 58.7   | 58.4                                   | 57.9   | 58.5    |
| 700         | 62.8                                  | —      | 62.1    | 63.4   | 62.5                                   | 60.3   | 61.8    |
| 800         | 67.9                                  | —      | —       | 68.0   | 67.7                                   | 65.3   | 65.4    |
| 900         | —                                     | —      | —       | 72.8   | 72.5                                   | 71.2   | 70.6    |
| 1000        | —                                     | —      | —       | 77.0   | 78.0                                   | 76.0   | 77.3    |
| 1100        | —                                     | —      | —       | 81.2   | 80.5                                   | —      | 79.1    |
| 1200        | —                                     | —      | —       | 85.1   | 83.7                                   | —      | 83.2    |
| 1300        | —                                     | —      | —       | 88.5   | 88.5                                   | —      | —       |
| 1400        | —                                     | —      | —       | 92.7   | 92.4                                   | —      | —       |

here at higher pressures ( $\geq 20$  cm of mercury) where the accommodation effect is negligibly small. The slopes of these linear plots (Fig. 3) in conjunction with thermal conductivity data [23] are interpreted on the basis of equation (6) to determine  $\alpha(T_H)$  with the results listed in Table 3B and graphed in Fig. 4B. The three sets of data do lead to consistent results thereby substantiating the constant temperature difference procedure of  $\alpha$  evaluation. Similarly, the  $\alpha$  values obtained for these three sets of data on the basis of equation (7) are displayed in Table 3C and Fig. 4C. In Table 3C, we also list  $T_H$  corresponding to each  $T_{L_i}$  and the gas pressures. For each of the three methods, the values of  $\alpha$  obtained from the three sets of measurements are graphically smoothed as shown by the continuous curves of Fig. 4.  $\alpha$  values read from these curves at round temperatures are tabulated in Table 3D to enable a quick comparison of the three methods of evaluating  $\alpha$  from data taken in the temperature-jump region.

#### EXPERIMENTAL VERIFICATION OF THE TEMPERATURE-JUMP THEORY

Since the above calculations of A.C.'s from the experimental data are based on the theory for the temperature-jump region, it is logical to ensure the correctness of the latter. Some evidence in support of this theory is already seen in the above two sections. Thus, we found that the qualitative requirement of theory for the pressure dependence of  $Q_H$  is substantiated by our measurements. We also checked the theory quantitatively, on the basis of equation (6) by computing  $k$  as a function of  $T$ , with good success. We report now the results of an additional quantitative check of the temperature-jump theory as given

by equation (5). This procedure is more general and covers a wider temperature range than the one based on equation (6).

The least-square analysis of the experimental data according to equation (5) leads to values of  $Q_H$  as a function of  $T_H$  for a constant  $T_w$  and corresponding to  $1/P = 0$ . A curve of  $Q_H$  vs  $T_H$  is then generated for each of the three sets of data and  $k$  is computed from the following relation [20, 23]:

$$k(T_H) = \frac{\ln(b/a)}{4\pi L} \left[ \frac{dQ_H}{dT_H} \right]. \quad (11)$$

Conductivity values thus obtained for the three sets of data over the entire temperature range are reported in the second half of Table 4 and these are in good agreement amongst each other, as well as with the mean values obtained from the measurements taken at a gas pressure of around 20 cm of mercury (outside the temperature-jump region) and equation (11). This check should be regarded both as comprehensive as well as conclusive for the experimental confirmation of the temperature-jump theory. In this background, the determination of A.C.'s according to the procedures described above must be regarded as based on a physical model which seems to assimilate at least all the essential features of heat transfer characterizing the temperature-jump region.

#### DISCUSSION

The A.C.'s values determined here are time independent as these are obtained from the steady state measurements when the wire surface is supposedly saturated or at least well-covered with the



gas for most of the test conditions. Figure 4 clearly shows that all the three sets of data lead to a very consistent set of  $\alpha$  values for a definite procedure, so that the geometry of the columns or the pressure range of measurements does not play any crucial role as long as these are properly chosen.

However, the three different methods of treatment of data taken in the temperature-jump region do lead to  $\alpha$  values which are only in fair agreement with each other. Several comments may be made to understand the trends explicitly clear in these sets of  $\alpha$  values. The correctness of equation (4), the constant power method, is implicit in equation (6), the constant temperature difference method. The fact that  $\alpha$  values as obtained by equation (6) are systematically greater than equation (4) then implies that the net effect of approximations made in developing the constant temperature difference method amounts to an overestimation of  $\alpha$ . It will appear that a careful determination of  $\alpha$  may have to improve upon several of the approximations made in deriving equation (6). It is noted that part of this discrepancy in  $\alpha$  values results because of the replacement of  $T_e$  in equation (6) by  $T_H$ . Further, both these methods employ the data of either  $Q_H$  or  $T_H$  at various  $P$  and lead to  $\alpha$  values as a function of  $T_H$ . In contrast the mean-free-path method generates  $\alpha$  values as a function of temperature at a constant gas pressure. It is for this reason that in Table 3C, the indication of  $P$  is essential unlike in Tables 3A and 3B. Further, though the practice has been to refer the  $\alpha$  values thus determined to  $T_L$ , we feel that a more appropriate choice is  $T_H$ . This will also bring in line a complete analogy between the mean-free-path and low pressure method. Both are based on the same physical model of the heat transfer at the wire surface. It may be remarked that if we qualitatively apply this correction to the  $\alpha$  values obtained from equation (7), which are already smaller than the values obtained from the two other methods, these will get further reduced. The net result would be that the agreement of  $\alpha$  values generated from equation (7) with those obtained from equations (4) and (6) will become worse than is evident in Table 3D. This should not be regarded at the present time as providing enough basis for the proper assessment of the mean-free-path method. We would like to emphasize the relative trends in the  $\alpha$  values as obtained according to the three methods. It may be pointed out that for both the constant temperature difference and the mean-free-path methods, the adequate knowledge of the temperature dependence of  $k$  on temperature is essential for  $\alpha$  evaluation.

We checked the mean-free-path method by the

computation of  $\alpha$  as a function of temperature at six different pressures (0.8, 1.05, 1.23, 1.43, 1.60 and 3.12 cm of Hg) from our data of Set II and found these values to be in good agreement with each other. This evidence will strongly substantiate the validity of the mean-free-path method. We feel that if such a check is confirmed by our more detailed measurements in progress, the basis of the mean-free-path method will be quite strongly founded. Conversely, these calculations also reveal that the surface of tungsten-nitrogen interface remains substantially unaltered as the nitrogen pressure is changed and that in  $\alpha$  we are referring to a reproducible interface property.

Theoretically speaking, the method based on equation (4) is preferable but this procedure reduces the temperature range for  $\alpha$  determined from the same initial data in comparison to the two other methods. We must, however, recall that all these three procedures for  $\alpha$  determination are valid only for a monatomic gas and consequently their use for nitrogen constitutes an overall approximation for the analysis procedure. We propose to undertake measurements on rare gases to shed light on this limitation and also follow up this work on polyatomic molecules to examine whether or not sufficiently different A.C. values are needed for the translational, rotational and vibrational modes [1]. However, if for the present we assume that the translational and internal degrees of freedom of a polyatomic gas are in equilibrium with each other, i.e. no relaxation effect, and further that a single A.C. can be employed for both translational and internal modes we get relatively simple expressions corresponding to equations (4), (6) and (7) which are as follows:

$$T_H - T_e = (Q_H/4\pi aLP)(\pi MT_e/2R)^{\ddagger} \times [4R/(2C_v + R)] [(2 - \alpha)/2\alpha] \quad (4a)$$

$$\frac{4\pi aL}{Q_H} = \frac{a \ln(b/a)}{k(\bar{T})(T_H - T_w)} + \frac{(2 - \alpha)(\pi MT_e)^{\ddagger}}{2\alpha P} \times \frac{4R}{(2C_v + R)} \frac{k(T_H)}{k(\bar{T})} \frac{1}{(T_H - T_w)} \quad (6a)$$

and

$$\alpha = \left(\frac{\pi M}{2R}\right)^{\ddagger} \left(\frac{4R}{2C_v + R}\right) \frac{Q_H T_L^{\ddagger}}{4\pi aLP(T_H - T_L)} \quad (7a)$$

where

$$T_L^{\ddagger} = \left(\frac{M}{128\pi R}\right)^{\ddagger} \left(\frac{4R}{2C_v + R}\right) \frac{Q_H}{bLP} \frac{1}{2} \left[ 4T_w + \frac{RMQ_H^2}{2\pi L^2 b^2 P^2 (R + 2C_v)^2} \right] \quad (10a)$$

and  $C_v$  is the specific heat of the gas at constant volume. For nitrogen we may assume  $C_v$  as equal to  $(5/2)R$  and the values of  $\alpha$  then obtained for the three procedures according to equations (4a), (6a) and (7a) are also reported in Table 3D. It will be noticed that these values are about 70 per cent of the values given by the expressions for a monatomic gas, i.e. equations (4), (6) and (7). It needs to be emphasized that the qualitative nature of the temperature dependence of  $\alpha$  remains completely undisturbed whether one assumes that the internal degrees of freedom of the gas molecules are frozen or not. This is an important result emerging from our present data.

A.C.'s values for nitrogen on tungsten are reported by Wachman [24] for filament temperatures in the range 344–516°K in the low pressure range as a function of pressure. Measurements at still higher temperatures are not available to the best of our knowledge. Present results and those of Wachman [24] are in good agreement with each other over the narrow overlapping temperature range. Roach and Thomas [15] reported A.C.'s for helium, neon and argon from data taken in the temperature-jump region up to a maximum temperature of  $T_e = 795^\circ\text{K}$ . Their conclusions concerning the relative use of the three procedures of equations (4), (6) and (7), are the same as elaborated above on the basis of current measurements. The qualitative dependence of  $\alpha$  on  $T$  as revealed by our measurements, Fig. 4, is to be noted as this suggests the presence of a minimum. However, this is not unique to nitrogen on tungsten only, and a similar trend is found in the data for helium on tungsten. Simple classical theories could be adjusted to reproduce such a dependence for helium on tungsten [4, 6, 7]. On the other hand, more detailed but primitive calculations [8–11] which include only some of the salient features of this complicated heat transfer process fail to reproduce even the qualitative temperature dependence of A.C. The art of theoretical manipulation has to go a long way before reliable wide range A.C. calculations will be possible. In this context the experimental efforts such as described here or that of Hanson [25] to determine A.C. employing a shock-tube become particularly promising both for engineering needs and to help develop a reliable base for the ab initio calculations in the near future.

*Acknowledgements* —This work is supported by the National Science Foundation under Grant No. GK-12519. We are thankful to Mr. W. M. Ross for his help in erecting this experimental facility and to Dr. J. P. Hartnett for his encouragement and interesting discussions. We are also grateful to Dr. F. O. Goodman for a critical reading of

this manuscript and for making several interesting suggestions.

## REFERENCES

1. R. G. Vines, The interchange of energy between molecules during collisions in the gas phase and at solid surfaces, *Rev. Pure Appl. Chem.* **4**, 207 (1954).
2. J. P. Hartnett, A survey of thermal accommodation coefficients, Rand Corporation, Research Memorandum RM-2585, 44 pp (19 March, 1960).
3. H. Y. Wachman, The thermal accommodation coefficient: a critical survey, *Am. Rocket Soc. J.* **32**, 2 (1962).
4. F. O. Goodman, On the theory of accommodation coefficients—III. Classical perturbation theory for the thermal accommodation of light gases, *J. Phys. Chem. Solids* **24**, 1451 (1963).
5. H. Shin, On the transfer of energy between a gas and a solid, *J. Phys. Chem.* **70**, 962 (1966).
6. F. O. Goodman and H. Y. Wachman, Formula for thermal accommodation coefficients, *J. Chem. Phys.* **46**, 2376 (1967).
7. F. O. Goodman, Classical theory of small energy accommodation coefficients. Application to  $^3\text{He}$  and  $^4\text{He}$  on W, *J. Chem. Phys.* **50**, 3855 (1969).
8. D. V. Roach and R. E. Harris, Modification of the Devonshire formula for the thermal accommodation coefficient of helium on tungsten, *J. Chem. Phys.* **51**, 3404 (1969).
9. F. O. Goodman and J. D. Gillerlain, Correction to the Devonshire theory of accommodation coefficients for bound-state transitions in gas-surface interactions, *J. Chem. Phys.* **54**, 3077 (1971).
10. J. R. Manson, Simple Model for the energy accommodation coefficient, *J. Chem. Phys.* **56**, 3451 (1972).
11. F. O. Goodman, One-phonon inelastic scattering of gas atoms in three dimensions by a simplified continuum mode of a solid: calculation of energy accommodation coefficients, *J. Chem. Phys.* **56**, 6082 (1972).
12. A. F. Devonshire, The interaction of atoms and molecules with solid surfaces. VIII—The exchange of energy between a gas and a solid, *Proc. R. Soc., Lond.* **158A**, 269 (1937).
13. H. Y. Wachman, Method for determining accommodation coefficients from data in the temperature-jump range without applying temperature-jump theory, *J. Chem. Phys.* **42**, 1850 (1965).
14. R. E. Harris, On the determination of thermal accommodation coefficients in the temperature-jump region, *J. Chem. Phys.* **46**, 3217 (1967).
15. D. V. Roach and L. B. Thomas, Determination of the thermal accommodation coefficients of gases on clean surfaces at temperatures above 300°K by the temperature-jump method, *Proc. Int. Symp. Rarefied Gas Dyn.* 5th, Vol. I, p. 163 (1967).
16. L. B. Thomas and R. C. Golike, A comparative study of accommodation coefficients by the temperature-jump and low-pressure methods and thermal conductivities of He, Ne and  $\text{CO}_2$ , *J. Chem. Phys.* **22**, 300 (1954).
17. G. L. Davis, Hot resistivity of tungsten wire, *Nature, Lond.* **196**, 656 (1962).
18. N. A. Ganti, S. H. P. Chen and S. C. Saxena, An experimental study of heat transfer through gases contained between two vertical coaxial cylindrical surfaces at different temperature, *Int. J. Heat Mass Transfer* **16**, 1589–1599 (1973).

19. S. H. P. Chen and S. C. Saxena, An analytical study of heat transfer through gases contained between two vertical coaxial cylindrical surfaces at different temperatures, to be published.
20. C. Saxena and F. E. Davis, Determination of thermal conductivity of gases at high temperatures: the column method, *J. Phys. E: Scient. Instrum.* **4**, 681 (1971).
21. E. H. Kennard, *Kinetic Theory of Gases*, pp. 331–327. McGraw-Hill, New York (1938).
22. R. D. Present, *Kinetic Theory of Gases*, pp. 190–193. McGraw-Hill, New York (1958).
23. S. C. Saxena, Transport properties of gases and gaseous mixtures at high temperatures, *High Temp. Sci.* **3**, 168 (1971).
24. H. Y. Wachman, Accommodation coefficients of nitrogen and helium on nitrogen covered tungsten between 325–496°K, *Proc. Int. Symp. Rarefield Gas Dyn.* 5th Vol. 1, 173 (1967).
25. R. K. Hanson, Shock-tube measurements of thermal accommodation, between a hot gas and a cold solid, Cranfield Institute of Technology, Cranfield Report Aero No. 2 (1970).

#### COEFFICIENTS DE TRANSFERT THERMIQUE ET D'ACCOMMODATION THERMIQUE INTERFACIAUX: FIL DE TUNGSTENE CHAUFFÉ DANS DE L'AZOTE

**Résumé**—On décrit un montage du type général à fil chaud réalisé pour étudier le transfert thermique interfacial entre les surfaces métalliques et un gaz environnant. Il s'agit d'analyser les différents mécanismes moléculaires de transport d'énergie qui s'établissent lors de la réduction progressive de la pression du gaz. En particulier on rapporte les flux thermiques mesurés pour le tungstène chauffé jusqu'à 1450 K dans de l'azote à des pressions variant entre 0,8 et 30 cm de mercure. Les mesures faites dans la région du saut de température sont interprétées selon trois voies. La théorie du saut de température est éprouvée avec succès en calculant la conductivité thermique et en la comparant avec les valeurs obtenues en fonction de la température à partir des mesures qui correspondent aussi bien à la région du saut de température qu'à la région externe. Les coefficients d'accommodation thermique sont ainsi obtenus pour l'azote sur une surface de tungstène avec un film adsorbé d'azote, pour un domaine de température compris entre 450 et 1450 K. Ces résultats rendront service aux ingénieurs parce que les conditions expérimentales correspondent à celles qui sont fréquemment rencontrées en pratique.

#### WÄRMEÜBERGANG UND THERMISCHE AKKOMODATIONSKOEFFIZIENTEN: BEHEIZTER WOLFRAMDRAHT IN EINER STICKSTOFFATMOSPHERE

**Zusammenfassung**—Es wird eine experimentelle Anordnung des allgemeinen Heizdraht-Typs beschrieben. Diese dient zur Untersuchung des Wärmeübergangs von einer beheizten Metalloberfläche in die umgebende Gasatmosphäre. Dabei sollen die verschiedenen molekularen Energietransportmechanismen erforscht werden, die sich bei allmählicher Erniedrigung des Gasdruckes einstellen. Speziell berichtet dieser Beitrag über den Wärmeübergang von Wolfram, das bis zu Temperaturen von 1450 K aufgeheizt wurde, an Stickstoff bei verschiedenen Drücken im Bereich von 8 bis etwa 300 mm Hg. Die Wärmeübergangsdaten, gewonnen im Bereich des Temperatursprunges, werden auf drei verschiedenen Wegen interpretiert. Die Theorie des Temperatursprunges wurde erfolgreich erprobt durch Berechnung und Vergleich der Werte der Wärmeleitung als Funktion der Temperatur, wobei diese Werte durch Daten innerhalb und ausserhalb des Temperatursprung-Bereiches gewonnen wurden. Die thermischen Akkomodationskoeffizienten für Stickstoff an eine Wolframoberfläche mit einem adsorbierten Film, bestehend hauptsächlich aus Stickstoff, wurden im Temperaturbereich von 450–1450 K ermittelt und ergeben ein schwaches Minimum bei etwa 850 K. Diese Daten werden einem Mangel bei ingenieurmässigen Berechnungen abhelfen, weil die Bedingungen der durchgeführten Experimente der in der Praxis meist auftretenden Konfiguration entsprechen.

#### КОЭФФИЦИЕНТ ПЕРЕНОСА ТЕПЛА И ТЕПЛОВОЙ АККОМОДАЦИИ НА ПОВЕРХНОСТИ РАЗДЕЛА ФАЗ: НАГРЕТАЯ ВОЛЬФРАМОВАЯ ПРОВОЛОКА В СРЕДЕ АЗОТА

**Аннотация**—Описывается конструкция прибора типа обычного проволочного термоанемометра, который используется для изучения процесса переноса тепла на границе раздела фаз от нагретых металлических поверхностей в окружающую газовую среду с целью выяснения различных молекулярных механизмов переноса энергии, которые задаются путем последовательного снижения давления газа. В частности, измерены скорости переноса тепла от вольфрама, нагретого до максимальной температуры 1450°K,

к азоту в диапазоне давлений от 0,8 до 30 см рт. ст. Данные по теплообмену, полученные в области скачка температуры, объясняются тремя различными способами. Теория температурного скачка проверялась с помощью мешинного счета и сравнением значений теплопроводности, полученных как функция температуры из данных, замеренных как в пределах, так и за пределами области температурного скачка. Таким способом получены значения коэффициента тепловой аккомодации для азота на поверхности вольфрамовой проволоки с адсорбированной пленкой, состоящей, в основном, из азота в диапазоне температур 450°–1450°K, которые свидетельствуют о том, что примерно при 850°K имеет место слабый минимум или провал. Таким образом, эти данные будут важны для инженерных расчетов, потому что условия эксперимента соответствуют конфигурациям, наиболее часто встречающимся на практике.